Int J Infrared Milli Waves (2007) 28:969–978
DOI 10.1007/s10762-007-9276-y

Effects of Scattering on THz Spectra of Granular Solids

Aparajita Bandyopadhyay · Amartya Sengupta · Robert B. Barat · Dale E. Gary · John F. Federici · Minghan Chen · David B. Tanner

Received: 15 May 2007 / Accepted: 24 July 2007 /
Published online: 17 August 2007

Abstract Experimental studies of granular solids have shown that significant scattering effects restrict the accurate determination of material absorption in the terahertz (THz) region. The present work investigates the grain size dependent scattering contribution on the extinction spectra of Ammonium Nitrate, flour and salt between 0.2 to 1.2 THz using THz time-domain spectroscopy. The scattering contribution can be estimated by applying Mie theory for spherical grains. The approach essentially separates the independent contributions of true absorption and scattering losses and thus determines the total extinction for different grain sizes of various materials. The separation of the intrinsic material absorption from scattering losses shows that the frequency dependence in weakly absorbing materials is predominantly particle size dependent. Consequently, that range of THz frequencies cannot be used to differentiate granular solids having no intrinsic absorption.

Keywords Terahertz · Spectroscopy · Granular solids · Extinction spectra · Material identification · Mie theory

1 Introduction

THz time-domain spectroscopy (THz-TDS) is one of the most promising candidates for non-contact and non-invasive studies of the optical parameters of different materials in the

A. Bandyopadhyay · A. Sengupta · D. E. Gary · J. F. Federici
Department of Physics, New Jersey Institute of Technology, Newark, NJ 07102, USA

R. B. Barat
Department of Chemical Engineering, New Jersey Institute of Technology, Newark, NJ 07102, USA

M. Chen · D. B. Tanner
Department of Physics, University of Florida, Gainesville, FL 32611, USA

A. Sengupta (✉)
Institute of Microwaves and Photonics, School of Electronic and Electrical Engineering
University of Leeds, Leeds LS2 9JT, UK
e-mail: A.Sengupta@leeds.ac.uk

far infrared region of the electromagnetic spectrum. It has been extensively employed to characterize the material parameters of various solids such as dielectrics, [1, 2] semiconductors, [3, 4] nanomaterials [5] and polymers. [6]

The allure of THz-TDS can be attributed to the facts that (a) coherent detection enhances the signal to noise ratio (SNR) of the measurement; (b) time resolved studies with subpicosecond time resolution is possible in the far-infrared region of the electromagnetic spectrum; and THz-TDS can record both the amplitude and phase simultaneously, thereby allowing the extraction of the optical properties of materials without resorting to the Kramers-Kronig relationships. [7]

In the study of solids, THz spectroscopy is particularly relevant as the observed absorption features could be linked to the states of crystallinity and morphological conditions of the solid under study. [8, 9] However, for solids having grain sizes comparable to THz wavelengths, the extinction spectra are greatly influenced by scattering losses which partially obscure the characteristic phonon resonances of the solids leading to complications in the quantitative analysis of the experimental data. [10, 11]

Since the THz extinction for finely ground solids does not vary as the fourth power of frequency, earlier reports have suggested that Rayleigh scattering can be ruled out. [8, 10] However, no corresponding theoretical model or quantitative estimation of the extinction of such granular materials has been reported even though some work has been reported on scattering of THz pulses to study propagation in random media. [12, 13]

Driven by the motivation of resolving the above limitations, we carried out THz spectroscopic measurements with Ammonium Nitrate, salt and flour. The identification of these materials is further complicated by their lack of having any sharp spectral signatures at lower THz frequencies. Fourier Transform Infrared (FTIR) studies have already reported that Ammonium Nitrate has a monotonically increasing attenuation spectra up to 3 THz. [14] Also, Kemp *et al*., [15] Zhang *et al*., [16] and Gallerano [17] have shown that flour and salt do not have any characteristic absorption features between 0.2 and 1.5 THz. These studies show that the extinction spectra is dependent on the size and refractive index of particles, however a quantitative verification has not been done. Therefore, the present study is conducted between 0.2 and 1.2 THz to inspect the effects of scattering on the spectra of these granular materials.

In this correspondence we report our experimental results and present an analytical treatment based on Mie scattering theory in the weak scattering limit by which we separate the effects of intrinsic material absorption and scattering losses and attempt to predict the frequency dependence of the extinction spectra for small grains in the weak scattering limit. This weak scattering limit is essentially the region where the principal interaction between THz radiation and the granular materials consist of single scattering events.

2 Experimental techniques

2.1 Experimental Set-up

The experimental set-up consists of a Ti:Sapphire laser emitting 125 fs pulses at 800 nm, part of which pumps a photoconductive substrate of semi insulating GaAs annealed at 600°C with a Hertzian dipole antenna microlithographically imprinted on it. This structure acts as a coplanar stripline (CPS) antenna when an AC bias is applied to it and becomes the source of THz radiation with a center frequency of about 0.5 THz.

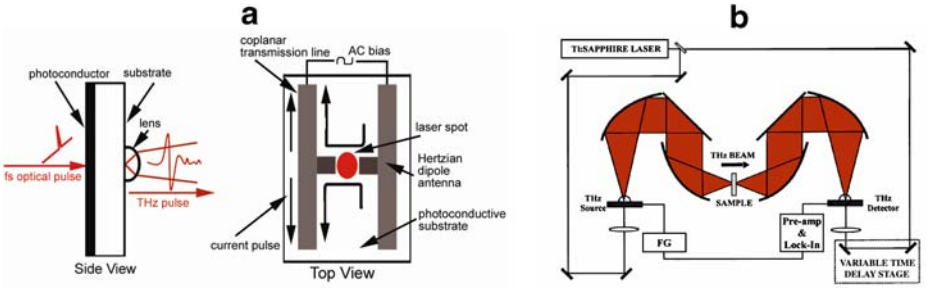

Fig. 1 (**a**) THz pulse generation from a photoconductive antenna structure. This is also known as Auston switch and its typical dimensions are Propagation of current pulses along the CPS structure is shown in top view. (**b**) THz spectroscopy set-up in transmission geometry.

The experimental set-up is shown in Fig. 1. The THz radiation from the source is guided through a set of gold plated off axis parabolic mirrors to the detector. The detection scheme is just the reverse of the generation process, where the incoming THz electric field provides the bias for the antenna which is optically gated by the other part of the laser pulse. The sample being studied is placed at the focus of the THz beam between two parabolic mirrors.

2.2 Sample preparation

Ammonium Nitrate (CAS # 6484-52-2, from Fischer Scientific®) having an average grain size of 700–750 μm was spread out uniformly in three sets of samples over Scotch® polyethylene packaging tape. The first set of the samples had a thickness of 1.602 mm. The next two sets were crushed using mortar and pestle to an average grain size of 350–400 μm, thickness: 0.380 mm and 100–150 μm, 0.413 mm respectively.

The salt sample (grain size~100–150 μm, thickness: 1.2 mm) was prepared from Shoprite® salt and the flour sample (grain size~150–200 μm, thickness: 0.8 mm) was prepared from commercially available Pillsbury® flour. Scotch® packaging tape was used as the sample holder and the two tapes sticking together was used as the reference or "blank" for the measurements. The standard procedure of making pellets mixed with high density polyethylene (HDPE) using a pellet press was avoided in order to maintain control over the grain sizes. Moreover, it has been reported that inexact mixing of PE powder and the compounds affects the absorption spectra. [27]

3 Spectroscopic investigation

3.1 Analysis of experimental data

On the basis of the general laws of absorption [18], we define the experimental extinction coefficient as a function of frequency,ν as:

$$\mu_{\exp}(\nu) = -\frac{\ln\left(\frac{|E_s(\nu)|^2}{|E_r(\nu)|^2}\right)}{w} \tag{1}$$

where $E_s(\nu)$ and $E_r(\nu)$ are the THz electric field components in the frequency domain corresponding to the sample and reference under study and w is the thickness of the sample. The THz fields in the frequency domain are obtained by performing a Discrete Fourier Transform (DFT) on the time domain data obtained experimentally.

Our earlier work has shown that the THz extinction of Ammonium Nitrate, flour and salt of different grain sizes rises slowly with frequency which does not follow Rayleigh scattering where a frequency dependence of the fourth power is expected. [10, 11, 19] Thus Mie theory which is more comprehensive in dealing with spherical grains of arbitrary size is considered for explaining this trend in the extinction spectra.

3.2 Theoretical modeling

The geometry of the incident and scattered fields is shown in Fig. 2. The perpendicular and parallel components of the electric field of the incident wave are $E_{ol} = \cos\varphi$, $E_{0r} = \sin\varphi$ and those of the scattered wave are $E_l = E_\theta$, $E_r = -E_\varphi$. Here r denotes the perpendicular component and l denotes the parallel component of the electric field.

Mie's formal solution for spheres of arbitrary size is given by, [20]

$$\left.\begin{aligned} E_\theta &= -\frac{i}{kr} e^{-ikr+i\omega t} \cos\varphi S_2(\theta) \\ E_\varphi &= \frac{i}{kr} e^{-ikr+i\omega t} \sin\varphi S_1(\theta) \end{aligned}\right\} \tag{2}$$

where $S_1(\theta)$ and $S_2(\theta)$ are two elements of the scattering matrix, $\mathbf{S}(\theta,\phi)$ and are known as amplitude functions, $k = 2\pi/\lambda$ is the wave number in vacuum and ω is the angular frequency. The radial components of the electric field are ignored as they tend to zero with higher powers of $1/r$.

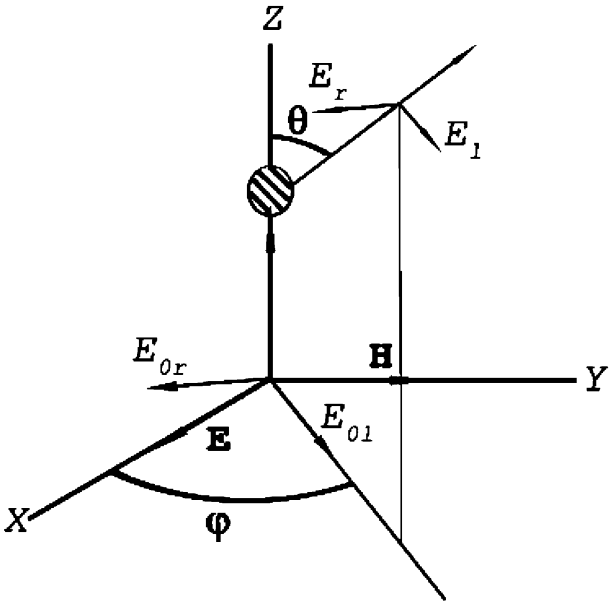

Fig. 2 Decomposition of electric vectors of incident and scattered waves. The plane of reference is taken through the directions of propagation of the incident and scattered waves. θ and φ are the polar and azimuthal angles respectively.

Considering that p-polarized THz radiation is incident on the samples, the theoretical extinction coefficient, μ_{th}, is calculated from the amplitude functions for $\theta=0$ ($S_1(\theta)$ *and* $S_2(\theta)$ are equal for $\theta=0$) and is given by,

$$\begin{aligned}\mu_{th} &= N\frac{c^2}{\pi\nu^2}\,\mathrm{Re}\,[S(0)] \\ &= N\frac{c^2}{2\pi\nu^2}\sum_{m=1}^{\infty}(2m+1)\,\mathrm{Re}\,(a_m+b_m)\end{aligned} \tag{3}$$

where N is the number of grains per unit volume, c is the speed of light and a_m, b_m are coefficients of the infinite summation such that,

$$\begin{cases} a_m = \dfrac{\psi_m'(y)\psi_m(x) - n\psi_m(y)\psi_m'(x)}{\psi_m'(y)\zeta_m(x) - n\psi_m(y)\zeta_m'(x)} \\ b_m = \dfrac{n\psi_m'(y)\psi_m(x) - \psi_m(y)\psi_m'(x)}{n\psi_m'(y)\zeta_m(x) - \psi_m(y)\zeta_m'(x)} \end{cases} \quad where \begin{cases} \psi_m(z) = zj_m(z) \\ \zeta_m(z) = zh_m^{(2)}(z) \end{cases} \tag{4}$$

Here $j_m(z)$ and $h_m^{(2)}(z)$ are Spherical Bessel functions of the first kind and third kind [21] respectively when z can be either $x=2\pi\nu r/c$ *or* $y=2\pi\nu n_r r/c$ and r is the radius of the spherical grain and n_r is the real refractive index. Eq. (3) is the theoretical equivalent of Eq. (1) and takes into account both the intrinsic absorption of the material as well as extrinsic losses involving single scattering events.

Mie theory also defines the complex refractive index of a scattering material $n(\nu)$ as, $n(\nu) = 1 - i2\pi NS(0)/k^3$. Equating the real and imaginary parts of this equation with $n(\nu) = n_r(\nu) + in_i(\nu)$, where $n_r(\nu)$ and $n_i(\nu)$ are the frequency dependent real and imaginary parts of the complex refractive index $n(\nu)$, one readily obtains,

$$\begin{aligned} n_i(\nu) &= \frac{2\pi N\,Re\,[S(O)]}{k^3} \\ &= \frac{\mu_{th}c}{4\pi\nu}\end{aligned} \tag{5}$$

which is the effective attenuation factor caused by the sum effect of material absorption and scattering losses, neglecting the effects of insignificantly small radiation pressure in the present case (it is inversely proportional to the velocity of light).

We can then separate the theoretical extinction coefficient μ_{th} into the coefficients of intrinsic material absorption μ_{abs} and scattering μ_{sca} as $\mu_{th}(\nu) = \mu_{abs}(\nu) + \mu_{sca}(\nu)$ where $\mu_{sca}(\nu)$ is given by,

$$\mu_{sca} = \frac{Nc^2}{2\pi\nu^2}\sum_{m=1}^{\infty}(2m+1)\left(|a_m|^2 + |b_m|^2\right) \tag{6}$$

In all of the above analysis, $n_r(\nu)$ can be assumed to be n_r, the frequency independent broadband refractive index, as all of the granular solids of the present study are known to have no sharp absorption features in the frequency range. This implies that there is no contribution of any intrinsic material absorption causing a sharp change in the value of the real part of the refractive index.

4 Results

4.1 THz time domain pulses and amplitude spectrum

In Fig. 3(a), typical THz electric field for the "blank" and for flour of 150–200 μm grain size has been shown. The corresponding amplitude spectrum is shown in Fig. 3(b) from which it is evident that the acceptable frequency range in our THz-TDS system is approximately between 0.2 and 1.2 THz. For reasons of repetition, corresponding plots obtained for other samples (Ammonium Nitrate of different grain sizes and salt) are not shown here.

From these time domain plots, the broadband refractive indices of the materials under study were calculated by observing the delay in the arrival of the THz pulse when the sample of finite thickness is placed between the source and the detector and was found to be 1.82, 1.54 and 1.44 for Ammonium Nitrate, salt and flour respectively which also agree with previously reported values. [8,9,22]

4.2 Comparison of Mie theory calculations with experimental analysis

The experimental extinction data for the different samples is shown in Fig. 4 with the theoretically calculated extinction curves up to the 4th order term in Eq. (4). In all the plots, Eq. (4) has been terminated at 4th order as it produces hardly any deviation as m changes value from 3 to 4. A comparison of the experimental and theoretical data for 700–750 μm Ammonium Nitrate shows a strong discrepancy in the 0.2–1.2 THz range and hence, has not been shown. It is believed that this is mainly due to the fact that the grains of these samples were mostly non spherical in shape.

The apparent roll off at higher frequencies as seen in Fig. 4 for all of the materials does not indicate any true phonon characteristic resonance but rather indicates the threshold of the region of validity of Mie theory. In other words, the fundamental assumption of Mie theory of single event scattering ceases to hold in higher frequency range as the incident wavelength becomes smaller compared to the size of the scatterers and their mutual separations leading to a dominance of multiple scattering events. [23] It is also observed that the experimental THz extinction of the materials with larger grain size (Ammonium Nitrate of 350–400 μm grain size) show significant deviation from the theory as any

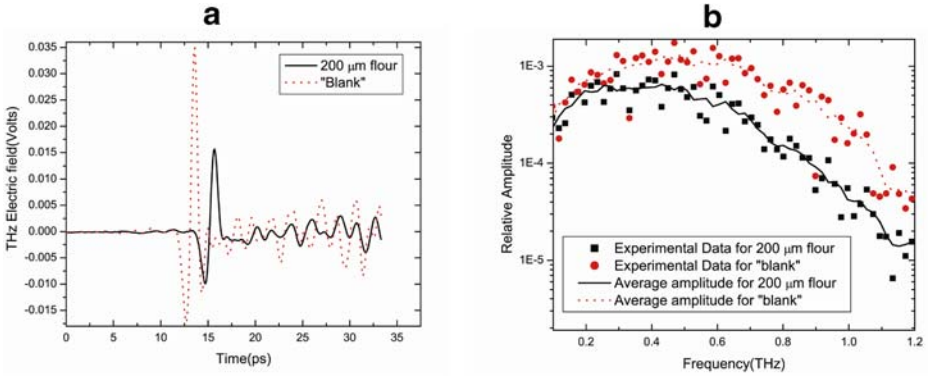

Fig. 3 (**a**) THz fields for 150–200 μm grain size flour and "blank" samples and (**b**) THz amplitudes of the same. The dips at 0.56, 0.78 and 1.13 THz are due to water vapor absorption. The "blank" was almost 95% transparent and completely featureless between 0.2 and 1.2 THz.

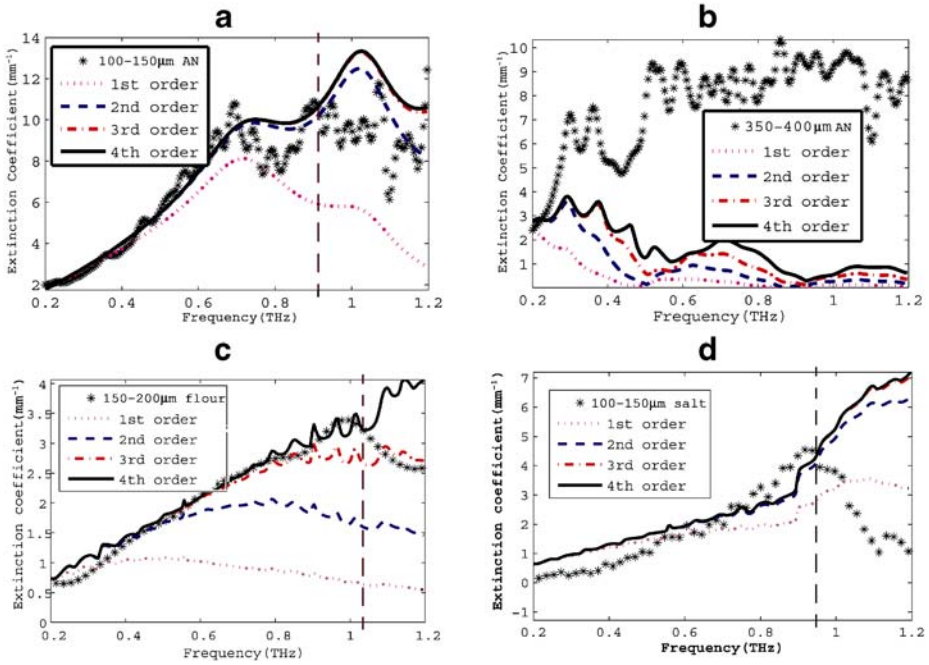

Fig. 4 Experimental and theoretical predictions of extinction coefficients for (**a**) 100–150 μm grain size Ammonium Nitrate, (**b**) 350–400 μm grain size Ammonium Nitrate, (**c**) 150–200 μm grain size flour and (**d**) 100–150 μm grain size salt. The red dotted line in parts (**a**), (**c**) and (**d**) shows the region upto which the prediction of Mie theory matches satisfactorily with the experimental analysis.

random irregularities of the spherical shape of the scatterers become prominent to the incident wavelength with larger grain sizes. Hence, for these large grain sizes, the weak scattering limit of the theory does not hold and other effects such as multiple scattering gain prominence. This contradicts the other assumption of our applied Mie theory which requires the scatterers to be spherical. In fact, on inspection of the samples with a microscope, it is found that the grains in the case of 100–150 μm Ammonium Nitrate, flour and salt are nominally spherical while the larger grains of Ammonium Nitrate form considerably irregular clusters.

4.3 Absorption and scattering coefficients

Figures 5(a) and (b) show the two parts of theoretically predicted extinction, that is, the intrinsic material absorption and extrinsic scattering losses, for the small grains of Ammonium Nitrate and salt using Eq. (6). For reasons of repetition, similar plots of flour have not been shown. It is seen that at lower frequencies, single event scattering is the predominant contribution towards the total extinction.

4.4 Identification of non absorbing spherical granular solids

From Fig. 4, it can be observed that all the materials investigated, namely Ammonium Nitrate, salt and flour have rising trends in their extinction spectra as observed experimentally which matches with the prediction of Mie theory in the limit of weak scattering, that is, in the region of lower THz frequencies. Provided that the spectral shape

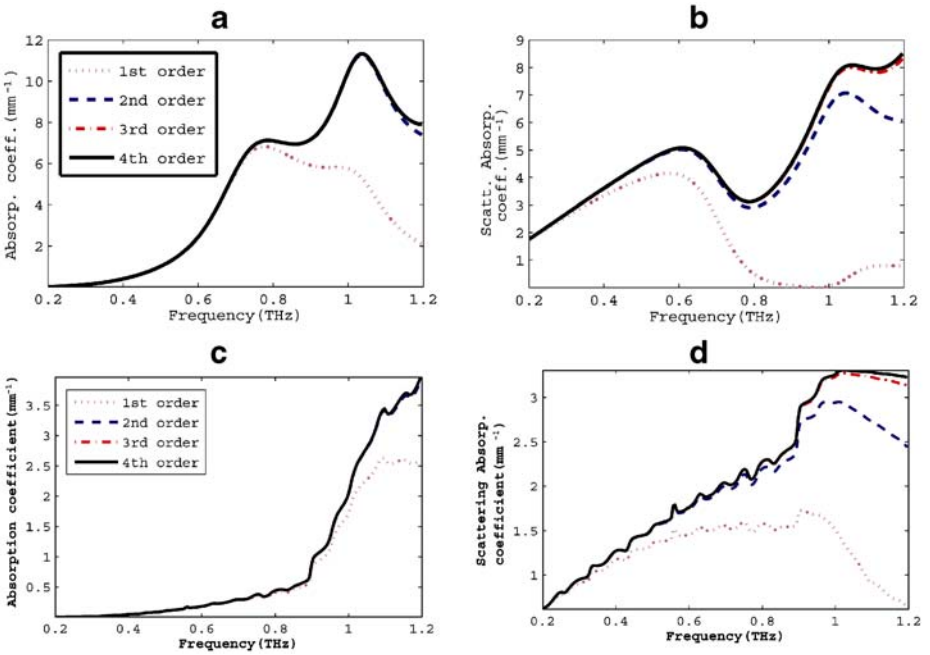

Fig. 5 Theoretically predicted absorption and scattering coefficients for (**a**) and (**b**) 100–150 μm Ammonium Nitrate and (**c**) and (**d**) 100–150 μm salt respectively. Similar legends have been followed for all the figures.

is characteristic of the material, previous reports have suggested that this might offer a possibility for spectral identification in the lower THz frequencies. [8, 9]

Therefore, to test the possibility, a generic curve based on Mie theory has been plotted which predicts the total extinction coefficient for different materials, M with refractive indices n_M, and a range of values of size parameter, x, to account for any variation of their size and/or wavelength as shown in Fig. 6(a). In the lower frequency region, the plot provides another incisive estimation of the total extinction for materials with a particular refractive index value and grain size, with respect to frequency. As shown in Fig. 6(b), (where the graph of Fig. 6(a) has been enlarged to show only upto the first undulation in the

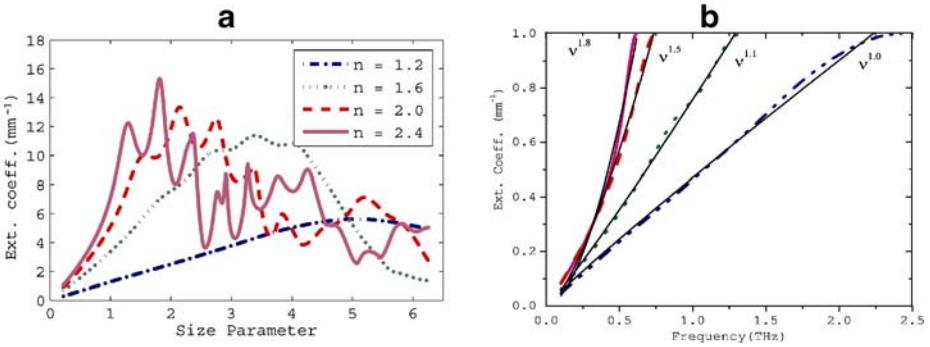

Fig. 6 Theoretically predicted extinction coefficients for materials having refractive indices, n and size parameters, x; and (**b**) the normalized extinction coefficient for a grain size of 100 μm as a function of frequency.

data), this becomes apparent when the different frequency dependences of the extinction coefficient are plotted for a constant grain size.

Hermann *et al*. [8] and Brown *et al*. [9] have reported experimental findings on absorption spectra of solid grains where they have shown the frequency dependence to be approximately ν^1 and ν^2 respectively, for flour (n~1.4) and sugar (n~2.0). Upon a direct comparison of these frequency trends with the theoretical plot of Fig. 6(b), we find that the predicted extinction spectra to be indeed $\nu^{1.0}$ and $\nu^{1.8}$ for those materials with those particular grain sizes. This effectively suggests that their observed spectra were primarily due to scattering contribution of the grains under study (flour~50 μm, sugar~300 μm).

Moreover, from Fig. 6(a) one can readily argue that these frequency trends are not unique or representative of the materials used. In fact, for a specific material with different grain sizes, one would obtain varying frequency dependence of extinction. Likewise, the grain sizes of different materials could be chosen in such a way that the extinction spectra of all those different materials with varying grain sizes would show a particular frequency trend. For example, 200 μm grains of flour and 450 μm grains of sugar would yield the same frequency trend of $\nu^{1.1}$ in the extinction spectra. Therefore, the frequency dependence of extinction spectra cannot be used for identifying non absorbing spherical granular solids of unknown grain sizes in the weak scattering region. Nonetheless, Figs. 6(a) and (b) also show that, in certain cases where the grain sizes are relatively known for a particular non-absorbing solid, the frequency trend of extinction spectra could be used for a broad classification of that solid since one can essentially estimate its refractive index.

5 Conclusions

In this study we experimentally obtain the extinction spectra of granular salt, flour and Ammonium Nitrate of different grain sizes between 0.2 to 1.2 THz using THz time domain techniques. We show that the obtained extinction for these materials in the frequency range of study essentially consist of scattering losses. We also demonstrate that Mie theory can be used in the weak scattering limit at THz region, but cannot be used for large non-spherical particle size. The intrinsic material absorption and scattering losses are separated from the total extinction and thus, the work makes an attempt to reconcile the apparent discrepancies in the extinction values of different materials of varying grain sizes by calculating the expected frequency dependence of such materials due to the impact of scattering. Finally, we also deduce from this study that any identification of an unknown solid in a concealed manner cannot be made based on the frequency trend of its THz extinction spectra, as the frequency dependence of the extinction of a solid is a function of both its material property, as well as its grain size.

Acknowledgements AS, AB, RBB, DEG and JFF gratefully acknowledge the funding support of the Technical Support Working Group, the Department of Homeland Security, and the US Army SBIR program. MC and DBT were supported by the NSF Condensed Matter Physics Program through grant DMR-0305043 and the DOE through DE-AI02-03ER46070.

References

1. C. J. Johnson, H. J. Sherman, and R. Weil, Far infrared measurement of the dielectric properties of GaAs and CdTe at 300K and 8K, Appl. Opt. **8**, 1667–1671 (1969).
2. K. Seeger, Microwave dielectric constants of silicon, gallium arsenide and quartz, J. Appl. Phys. **63**, 5439–5443 (1988).

3. D. Grischkowsky, S. Keiding, M. V. Exter, and Ch. Fattinger, J. Opt. Soc. Am. B. **7**, 2006–2015 (1990).
4. T. D. Dorney, R. G. Baraniuk, and D. M. Mittleman, Material parameter estimation with terahertz time-domain spectroscopy, J. Opt. Soc. Am. A. **18**, 1562–1571 (2001).
5. H. Altan, F. Huang, J. F. Federici, A. Lan, and H. Grebel, Optical and electronic characteristics of single walled carbon nanotubes and silicon nanoclusters by terahertz spectroscopy, J. Appl. Phys. **96**, 6685–6689 (2004).
6. A. Sengupta, A. Bandyopadhyay, B. F. Bowden, J. A. Harrington, and J. F. Federici, Characterization of olefin copolymers using terahertz spectroscopy, Electron. Lett. **42**, 1477–1479 (2006).
7. C. Kittel, Solid State Physics, (John Wiley and Sons, New York, 1998).
8. M. Hermann, M. Tani, M. Watanabe, and K. Sakai, Terahertz imaging of objects in powders, IEE Proc.-Optoelectronics. **149**, 116–120 (2002).
9. T. L. J. Chan, J. E. Bjarnason, A. W. M. Lee, M. A. Celis, and E. R. Brown, Attenuation contrast between biomolecular and inorganic materials at terahertz frequencies, Appl. Phys. Lett. **85**, 2523–2525 (2004).
10. P. F. Taday, Applications of terahertz spectroscopy to pharmaceutical sciences, Philosophical Transactions of the Royal Society of London A. **362**, 351–364 (2004).
11. A. Sengupta, A. Bandyopadhyay, R. B. Barat, D. E. Gary, and J. F. Federici, Study of morphological effects on terahertz spectra using ammonium nitrate in *Optical Terahertz Science and Technology Topical Meeting on CD ROM* (The Optical Society of America, Washington D.C. 2005) **ME6.**
12. J. Pearce, and D. M. Mittleman, Using terahertz pulses to study light scattering, Physica B. **338**, 92–96 (2003).
13. K. J. Chau, G. D. Dice, and A. Y. Elezzabi, Coherent plasmonic enhanced terahertz transmission through random metallic media. **94**, 173904 (2005).
14. J. F. Federici, B. Schulkin, F. Huang, D. E. Gary, R. B. Barat, F. Oliviera, and D. Zimdars, THz Imaging and Sensing for security applications, Semiconductor Science and Technology. **20**, S266–S280 (2005).
15. M. C. Kemp *et al*, Security applications of terahertz technology, in *Terahertz for Military and Security Applications,* R. Jennifer Hwu (ed), Proc. SPIE. **5070**, 44–52 (2003).
16. B. Ferguson, S. Wang, H. Zhong, D. Abbott, and X.-C. Zhang, Powder detection with T-ray imaging, in *Terahertz for Military and Security Applications,* R. Jennifer Hwu (ed), Proc. SPIE. **5070**, 7–16 (2003).
17. G.P. Gallerano, "THz Spectroscopic Database," at http://www.frascati.enea.it/THz-BRIDGE (2004).
18. M. Born, and E. Wolf, Principles of Optics, (Cambridge University Press, London, 1999).
19. A. Bandyopadhyay, A. Sengupta, R. B. Barat, D. E. Gary, and J. F. Federici, Grain size dependent scattering studies of common materials using THz time domain techniques, in *Terahertz and Gigahertz Electronics and Photonics V,* R. Jennifer Hwu (ed), *Proc. SPIE* **6120**, 61200H (2006).
20. H. C. Van de Hulst, Light scattering by small particles, (Dover Publications, New York, 1981).
21. M. Abramowitz, and I. A. Stegun, Handbook of Mathematical Functions, with Formulas, Graphs and Mathematical Tables, (Dover Publications, New York, 1974).
22. M. A. Jarzembski, M. L. Norman, K. A. Fuller, V. Srivastava, and D. R. Cutten, Complex refractive index of ammonium nitrate in the 2–20 μm spectral range, Appl. Opt. **42**, 922–930 (2003).
23. C. Dodson, M.J. Fitch, R. Osiander and J.B. Spicer, Terahertz imaging for anti-personnel mine detection, in *Terahertz for Military and Security Applications III*, R. Jennifer Hwu, (ed), Proc. SPIE. **5790**, 85–93 (2005).